Range of electrons and positrons in matter

R. K. Batra
Physics Department, Punjab Agricultural University, Ludhiana-141004, Punjab, India

M. L. Sehgal
Physics Department, Aligarh Muslim University, Aligarh, India

(Received 27 March 1979; revised manuscript received 14 March 1980)

The practical ranges of electrons and positrons of kinetic energy ranging from 0.25 to 5.0 MeV are calculated considering their total inelastic and the multiple Coulomb elastic scattering with the atomic and the nuclear fields of the atoms of an absorbing material. The electrons and positrons are assumed to travel along the direction of incidence until they lose energy to the extent that the calculated mean-square projected angle due to the multiple scattering, on the plane containing the initial direction, becomes so large that their further motion becomes random. The random motion contributes to straggling only. The calculated ranges of electrons and positrons are found to explain satisfactorily the energy dependence and the material dependence of the experimental extrapolated ranges. The ratio of the measured positron range at 1.88 MeV to electron range at 1.77 MeV in Al, Cu, Sn, Yb, and Pb agrees well with the calculation. But there is a large difference in the calculated and experimental ratio of positron to electron range in some rare-earth elements and graphite.

I. INTRODUCTION

Many measurements[1–10] on the transmission of electrons and positrons in different materials have been reported since the discovery of radioactivity. A comprehensive summary of the experimentally obtained ranges of 59 monoenergetic electron energies and 35 continuous β-ray energies has been reported by Katz and Penfold.[5] The measured transmitted intensity versus thickness curves have been utilized to estimate the ranges of electrons and positrons employing various definitions of range such as the extrapolated range, the maximum range, the average range, etc. Among them, the extrapolated range denoted by R_{ex} is most commonly used. The most generalized semiempirical equation for the extrapolated range of electrons in different absorbers has been published by Tabata *et al.*[11] The data on positron transmission are scarce relative to the electron-transmission meaurements. However, Takhar[12–14] reported the ratio of the measured positron range R_{ex}^{+} to that of electron's R_{ex}^{-} of nearly the same energy (around 1.8 MeV) and concluded that R_{ex}^{+}/R_{ex}^{-} increases systematically with the atomic number of the metallic absorbers.

Surprisingly enough, a very few theoretical investigations have been made to understand systematically the range of electrons and positrons in various absorbers. In 1964, Berger and Seltzer[15] computed the continuous slowing down approximation (csda) ranges of electrons and positrons, denoted as R^{-} and R^{+}, respectively, by integrating numerically the reciprocal of the total energy-loss expressions under the continuous slowing down approximation [see Eq. (1) for definition]. The simplified expressions of the csda range of electrons and positrons based upon the empirical relations of total stopping power have been reported by us.[16–18] The csda range R^{-} and the extrapolated range R_{ex}^{-} versus the energy of electron for the absorber of Al, Cu, and Au are shown in Fig. 1. The study of Fig. 1 reveals that the csda range increases with the energy of electron and the atomic number of the absorber. While, on the other hand, the data on extrapolated ranges indicate that R_{ex}^{-} is an

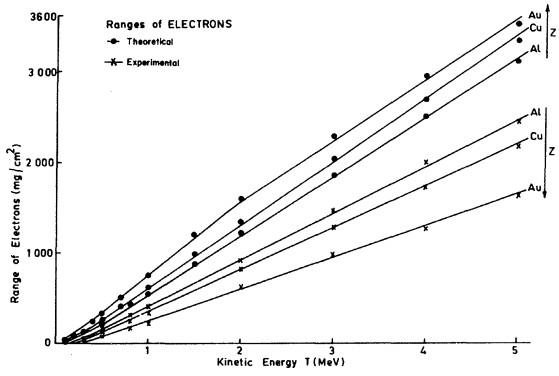

FIG. 1. csda range R and the extrapolated range R_{ex} of electron versus energy for aluminum, copper, and gold.

increasing function of the electron's energy and decreasing function of atomic number of the absorber. Hence, we learn that the csda range of electron is not a suitable quantity to understand the extrapolated ranges of electron in different materials. Similar trends of comparison between the calculated R^+ and the few measured values of R_{ex}^+ for positrons have been observed.[7,10,15]

As some more information on positron transmission[10,19] and the difference in electron and positron penetrations in materials[12–14] has appeared during the last decade, there is a need to reexamine the penetration behavior of electrons and positrons through matter. In this paper, we present a method of calculating the practical range of electrons and positrons denoted by R_p^- and R_p^+, respectively, by taking into account the total stopping power[16–18] in conjunction with their multiple scattering.[20–23] The method is confined to the energy region from 0.25 to 5.0 MeV, where numerous extrapolated ranges of electrons and relatively few measurements of positrons are available. The calculated practical ranges of electrons and positrons are compared with the existing data on R_{ex}^- and R_{ex}^+ and the results are discussed in detail.

II. METHOD OF CALCULATION

The fact that the electrons and positrons, on passage through matter, interact with the atoms of an absorber, inelastically as well as elastically is utilized to determine the practical range of electrons and positrons. The method accounts for the effect of multiple Coulomb elastic scattering on the csda range calculated from the total stopping power only.[15,18] The present method depends upon the following assumptions:

(i) It is assumed that the electrons and positrons move approximately in straight paths along the direction of incidence, by undergoing inelastic interactions only, and the deviation of their path due to multiple elastic scattering is ignored from the considerations at the first instant. Consequently, the particles (e^- or e^+) would go on losing energy while traversing along the original direction, until they come to rest completely (see Fig. 2). Therefore, the range of electrons and positrons[15] of kinetic energy T, under the continuous slowing down approximation is given as

$$R^{\pm}(T)=\int_0^T\left[\left(\frac{dE}{dx}\right)_{\text{tot}}^{\pm}\right]^{-1}dE \ , \tag{1}$$

where dE/dx is the sum of the energy loss due to collisions (ionization plus excitation loss) and that due to bremsstrahlung. The upper and the lower superscripts stand for positrons and electrons, respectively.

(ii) Actually, the particle's path deviates due to the multiple-scattering process, especially near the end of their journeys. Therefore, we further assume that electrons and positrons move approximately in the direction of incidence until they lose their energy to the extent for which the calculated mean-square projected angle due to multiple scattering on the plane containing the initial direction becomes very large. Thereafter, the particles lose their memory of the original direction; i.e., they begin to move randomly. For instance, a typical case of penetration is depicted in Fig. 2. The situation of random motion of electrons and positrons is physically realized by making use of the definition of mean transport free path.

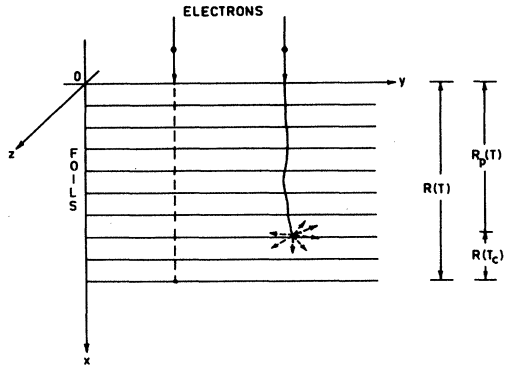

FIG. 2. Typical case of penetration of electrons (or positrons) through thin metallic foils. The dotted line corresponds to the range considering inelastic interactions only, while the full line indicates the range considering both inelastic and elastic interactions.

Let T_c^+ and T_c^- represent, respectively, the characteristic energy of positrons and electrons of energy T, relating to the situation when positrons and electrons just begin to undergo random motion. Assuming that the random motion contributes to straggling only, the mean practical range R_p^+ of positron and R_p^- of electron is given by

$$R_p^{\pm}(T)=R^{\pm}(T)-R^{\pm}(T_c^{\pm}) \ , \tag{2}$$

where $R^{\pm}$ can be obtained from Eq. (7) of Ref. 18. The method of calculating T_c^+ and T_c^- is described below.

A. Calculation of $T_c^{\pm}$

For the determination of $T_c^{\pm}$, we require the knowledge of the mean-square projected angle due to multiple scattering of these particles on the plane containing the incidence beam. Many workers[21,24,25] have derived the expression for the mean-square angle of electron scattering using Rutherford's scattering formula.[21] Among the various review articles on multiple scattering of electrons, Williams review[25] on

multiple scattering of electrons presents a complete picture of all the theories. However, for the sake of the mathematical convenience in the present problem, we use Williams theory[21] of small angles multiple scattering in conjunction with Mott's[20] and Massey's[22] scattering cross section for e^- and e^+, respectively, as modified to include the screening of nuclear charge by the orbital electrons.

Let the resultant deflection of the subsequent scatterings of electrons and positrons passing through a foil of thickness dx be θ and let Φ represent its projection on the plane containing the initial direction. While dealing with the multiple scattering of fast electrons, Williams[21] had shown that the small angle multiple scattering yields a Gaussian distribution and, according to this theory (see Sec. 2 of Ref. 21), the mean-square scattering angle is given as

$$\langle\theta^2\rangle^{\pm}_{dx}=\frac{N\,dx}{\pi}\int_{\theta_s}^{\pi}\theta^2\sigma_{\pm}(\theta,\gamma)2\pi\theta\,d\theta\ , \tag{3}$$

where N is the number of nuclei per cm^3, γ the kinetic energy of incident electrons or positrons in units of the rest mass energy of an electron, $\sigma_{\pm}(\theta,\gamma)$ the elastic scattering cross section for e^+ and e^-, and θ_s the screening angle.[21] The elastic scattering cross section for electrons[20] and positrons[22] as expanded by McKinley and Feshbach[23] in powers of αZ (α being the fine-structure constant and Z the atomic number of a scatterer) is given by

$$\sigma_{\pm}(\theta,\gamma)=\frac{1}{4}\frac{r_0^2Z(Z+1)}{(\gamma^2-1)^2}\frac{1}{\sin^4(\frac{1}{2}\theta)}\left[1-\frac{\gamma^2-1}{\gamma^2}\sin^2\tfrac{1}{2}\theta\mp\frac{\pi\alpha Z(\gamma^2-1)^{1/2}}{\gamma}\sin\tfrac{1}{2}\theta(1-\sin\tfrac{1}{2}\theta)+\cdots\right]\ , \tag{4}$$

where r_0 is the electron radius. Further, it can be shown using Fermi-Thomas distribution[21] that the elastic scattering cross section is cut off for the angles smaller than $\theta_s=\alpha Z^{1/3}(\gamma^2-1)^{1/2}$.

While deriving the expression for $\langle\theta^2\rangle$ for fast electrons, Williams[21] and Rossi *et al.*[24] considered only the first term of Eq. (4), which represents Rutherford scattering formula.[25] Later, Hereford and Swann[2] used the same expression in their semiempirical approach to explain the extrapolated ranges of 3.0- to 12.0-MeV electrons in Al and Cu. Clearly, such formulas for $\langle\theta^2\rangle$ do not distinguish electrons from positrons. It is apparent from Eq. (4) that the positron scattering is always less than the electron scattering under the identical conditions. The third term in the square brackets of Eq. (4) gives the difference between positron and electron scatterings and is very important for absorbers of high atomic number. Therefore, it is significant to use Eq. (4) as a whole to understand the difference in penetration of positrons from that of electrons, particularly in the materials of high atomic numbers. Now, we substitute Eq. (4) into Eq. (3) and integrating over θ, one finds

$$\langle\theta^2\rangle^{\pm}_{dx}=8Nr_0^2Z(Z+1)\frac{\gamma^2}{(\gamma^2-1)^2}(dx)^{\pm}\left[\ln\frac{2(\gamma^2-1)^{1/2}}{\alpha Z^{1/3}}-\frac{1}{2}\frac{\gamma^2-1}{\gamma^2}\mp\frac{\pi\alpha Z(\gamma^2-1)^{1/2}}{\gamma}\left(1-\frac{\alpha Z^{1/3}}{(\gamma^2-1)^{1/2}}\right)+\cdots\right]\ . \tag{5}$$

When the thickness penetrated by the electrons and positrons is finite, the total energy loss must be included in the calculation of $\langle\theta^2\rangle^{\pm}$. To do so, we substitute the values of $(dx)^{\pm}$ from the empirical relation[18] of total stopping power into Eq. (5), integrating over γ and simplifying, we find

$$\langle\theta^2\rangle^{\pm}_{(\gamma-\gamma_c)}=\frac{8Nr_0^2Z(Z+1)m_1c^2}{\rho(m_1Z+c_1)}\left[\ln\left(\frac{2}{\alpha Z^{1/3}}\right)(I_1-I_2^{\pm})+\tfrac{1}{2}(I_3-I_4^{\pm}-I_5+I_6^{\pm})\right.$$
$$\left.\mp\tfrac{1}{2}\pi\alpha Z(I_7-I_8^{\pm})\pm\tfrac{1}{2}\pi\alpha^2Z^{4/3}(I_9-I_{10}^{\pm})\right]_{\gamma_c}^{\gamma}\ , \tag{6}$$

where γ and γ_c represent, respectively, the incident kinetic energy of e^- or e^+ and its energy at any instant of penetration. Here, the constants m_1 and c_1 correspond to the constants m and c of Ref. 18. The

integrals involved in Eq. (6) are given below

$$I_1=\int \frac{d\gamma}{(\gamma^2-1)^2},\quad I_2^{\pm}=\int \frac{\gamma^{(a^{\pm}Z+b^{\pm})}}{(\gamma^2-1)^2}\,d\gamma\ ,$$

$$I_3=\int \frac{\ln(\gamma^2-1)}{(\gamma^2-1)^2}\,d\gamma\ ,$$

$$I_4^{\pm}=\int \frac{\gamma^{(a^{\pm}Z+b^{\pm})}\ln(\gamma^2-1)}{(\gamma^2-1)^2}\,d\gamma\ ,$$

$$I_5=\int \frac{d\gamma}{\gamma^2(\gamma^2-1)},\quad I_6^{\pm}=\int \frac{\gamma^{(a^{\pm}Z+b^{\pm}-2)}}{(\gamma^2-1)}\,d\gamma\ ,$$

$$I_7=\int \frac{d\gamma}{\gamma(\gamma^2-1)^{3/2}},\quad I_8^{\pm}=\int \frac{\gamma^{(a^{\pm}Z+b^{\pm}-1)}}{(\gamma^2-1)^{3/2}}\,d\gamma\ ,$$

$$I_9=\int \frac{d\gamma}{\gamma(\gamma^2-1)^2},\quad I_{10}^{\pm}=\int \frac{\gamma^{(a^{\pm}Z+b^{\pm}-1)}}{(\gamma^2-1)^2}\,d\gamma\ .$$

The constants $a^{\pm}$ and $b^{\pm}$ are given in Ref. 18.

As we are interested in the mean-square projected deflection, we write below the expression for $\langle\Phi^2\rangle$, by making use of the standard relation,[21] viz., $\langle\Phi^2\rangle=\frac{1}{2}\langle\theta^2\rangle$:

$$\langle\Phi^2\rangle^{\pm}_{(\gamma-\gamma_c)}=-D[F^{\pm}(\gamma)-F^{\pm}(\gamma_c)]\ , \tag{7}$$

for $0.25\leq T\leq 5.0$ MeV, where

$$D=\frac{4Nr_0^2Z(Z+1)m_lc^2}{\rho(m_1Z+c_1)}$$

and

$$F^{\pm}(\gamma)=\ln(2/\alpha Z^{1/3})(I_1-I_2^{\pm})+\tfrac{1}{2}(I_3-I_4^{\pm}-I_5+I_6^{\pm})\mp\tfrac{1}{2}\pi\alpha Z(I_7-I_8^{\pm})\pm\tfrac{1}{2}\pi\alpha^2Z^{4/3}(I_9-I_{10}^{\pm})\ . \tag{8}$$

The functions $F^+(\gamma)$ and $F^-(\gamma)$ indicate the interplay of the elastic and inelastic processes of positrons and electrons, respectively, upon their penetrations through a known absorber of some finite thickness.

Further, the mean-square multiple-scattering angle in terms of cross section $\sigma_{\pm}(\theta,\gamma)$ is given as

$$\langle\theta^2\rangle^{\pm}_{dx}=2(dx)^{\pm}\int\sigma_{\pm}(\theta,\gamma)(1-\cos\theta)\,d\Omega\ , \tag{9a}$$

where $d\Omega$ is an elementary solid angle.

To visualize the situation of the random motion of positrons and electrons due to multiple scattering, we use the definition of transport mean free path and write Eq. (9a) as

$$\langle\theta^2\rangle^{\pm}_{dx}=\frac{2(dx)^{\pm}}{\lambda_t^{\pm}}\ , \tag{9b}$$

where λ_t^+ and λ_t^- represent the transport mean free paths of positrons and electrons, respectively. Now, equating Eqs. (5) and (9b) and solving for $\lambda_t^{\pm}$, we have

$$\lambda_t^{\pm}=2\left\{8Nr_0^2\frac{Z(Z+1)}{\gamma^2-1}\gamma^2\left[\ln\left(\frac{2(\gamma^2-1)^{1/2}}{\alpha Z^{1/3}}\right)-\frac{1}{2}\left(\frac{\gamma^2-1}{\gamma^2}\right)\mp\frac{\pi\alpha Z}{\gamma}(\gamma^2-1)^{1/2}\left(1-\frac{\alpha Z^{1/3}}{(\gamma^2-1)^{1/2}}\right)\right]\right\}^{-1}\ . \tag{10}$$

Therefore, the mean-square angle relating to the characteristic random motion, is given by

$$\langle\theta_c^2\rangle^{\pm}=\int_0^{\lambda_t^{\pm}}8Nr_0^2Z(Z+1)\frac{\gamma^2}{(\gamma^2-1)}\left[\ln\left(\frac{2(\gamma^2-1)^{1/2}}{\alpha Z^{1/3}}\right)-\frac{1}{2}\left(\frac{\gamma^2-1}{\gamma^2}\right)\mp\frac{\pi\alpha Z(\gamma^2-1)^{1/2}}{\gamma}\left(1-\frac{\alpha Z^{1/2}}{(\gamma^2-1)^{1/2}}\right)\right]d\gamma\ . \tag{11}$$

From Eqs. (10) and (11), it follows that

$$\langle\theta_c^2\rangle^{\pm}=2,\quad\langle\Phi_c^2\rangle^{\pm}=1\ . \tag{12}$$

Therefore, inserting this into Eq. (7), we have

$$F^{\pm}(\gamma_c^{\pm})=F^{\pm}(\gamma)+D^{-1}\ . \tag{13}$$

B. Computation

The values of $F^-(\gamma)$ and $F^+(\gamma)$ versus energy (from 0.2 to 5.0 MeV) for the absorbers of atomic number $Z=1$ to 92 have been obtained using a computer. The plots of $F^-(\gamma)$ and $F^+(\gamma)$ versus energy for Al and Au are shown in Figs. 3 and 4, respectively. The behavior of $F^{\pm}(\gamma)$ versus energy for other elements is similar to that of Figs. 3 and 4. It is found that the difference between $F^-(\gamma)$ and $F^+(\gamma)$

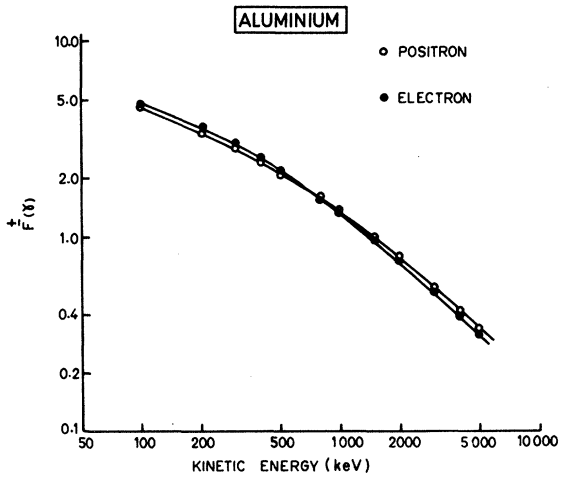

FIG. 3. Calculated values of $F^{\pm}(\gamma)$ vs kinetic energy of electron (●) and positron (○) in aluminum.

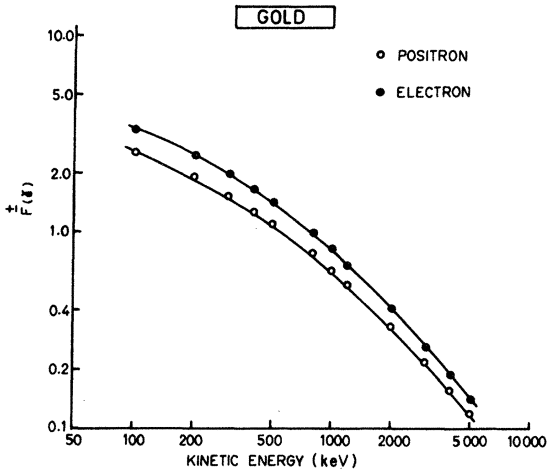

FIG. 4. $F^{\pm}(\gamma)$ vs kinetic energy in gold. Figure caption is the same as Fig. 3.

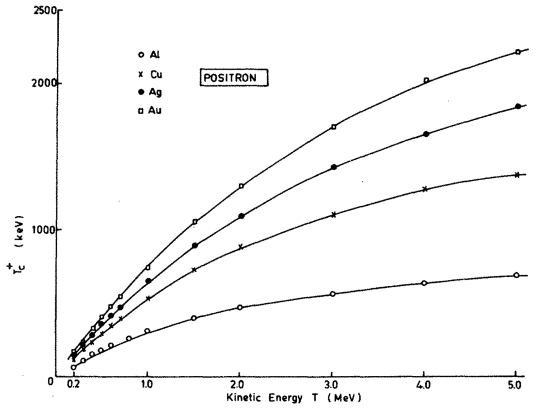

FIG. 6. Estimated values of T_c^+ vs kinetic energy of positron in Al, Cu, Ag, and Au.

increases systematically with atomic number. This trend indicates the large reduction in the csda ranges of e^- and e^+ due to multiple scattering in the case of heavy elements compared to the light elements.

Now using Eq. (13) and the plot of $F^{\pm}(\gamma)$ versus energy for a given atomic number, the values of T_c^+ and T_c^- can be obtained for a given energy. Thus, knowing T_c^+ and T_c^- for a given energy, the practical ranges R_p^+ of positron and R_p^- of electron may be computed using Eq. (2) and its associated equations in Ref. 18. For the sake of completeness, the computed values of T_c^- and T_c^+ versus energy for different materials are displayed in Figs. 5 and 6, respectively.

III. RESULTS AND DISCUSSION

Table I contains the practical ranges of electron of energy from 0.25 to 5.0 MeV in Al, Cu, Ag, and Au as calculated by the present method, along with the values of R_{ex}^- for electrons estimated due to the semiempirical approach of Tabata *et al.*[11] It is apparent from Table I that our method explains nicely the dependence of the measured electron ranges on the atomic number of the absorbing material and the electron energy. Furthermore, it is clear from Fig. 7 that the calculated practical range R_p^+ of positron is a decreasing function of atomic number. As the measurements on positron ranges are sparse and even some workers[6,19,26] did not extract the range of positron from their measured transmission data, the direct comparison like that of the electrons shown in

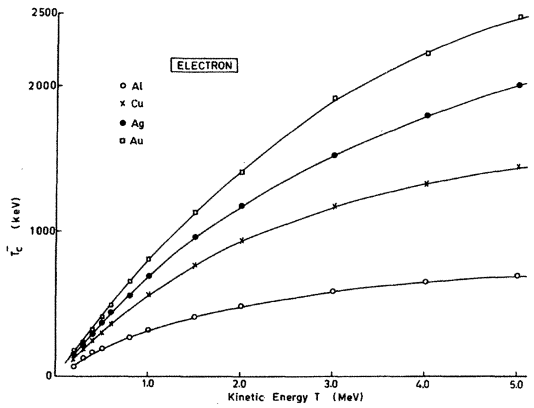

FIG. 5. Estimated values of T_c^- vs kinetic energy of electron in Al, Cu, Ag, and Au.

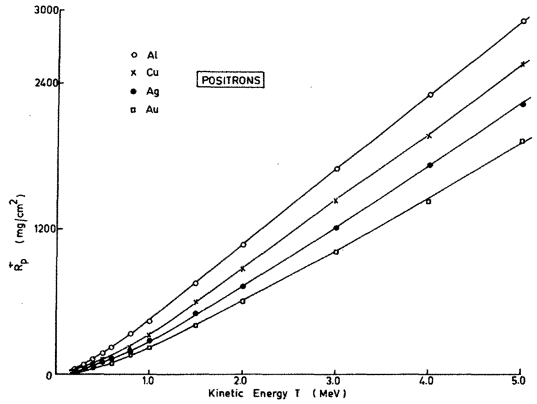

FIG. 7. Calculated range R_p^+ of positron in mg/cm^2 according to Eq. (2) as a function of energy for the absorbers aluminum (○), copper (×), silver (●), and gold (□).

TABLE I. Comparison between the calculated R_p^- (this work) and the extrapolated range (Ref. 11) of electron in Al, Cu, Ag, and Au at various energies. The ranges are expressed in mg/cm^2.

Kinetic energy (MeV)	Aluminum Expt. R_{ex}^-	Calc. R_p^-	Copper Expt. R_{ex}^-	Calc. R_p^-	Silver Expt. R_{ex}^-	Calc. R_p^-	Gold Expt. R_{ex}^-	Calc. R_p^-
0.25	57.6 ± 4.8	62.3	47.9 ± 2.4	44.3	40.7 ± 3.8	36.3	29.1 ± 2.9	26.2
0.30	77.8 ± 5.1	82.2	60.7 ± 3.0	57.9	51.2 ± 4.8	49.2	39.0 ± 5.4	31.5
0.40	114.7 ± 7.4	124.2	94.5 ± 4.7	89.9	80.8 ± 7.6	71.8	59.8 ± 8.2	51.2
0.50	158.2 ± 10.3	167.3	131.5 ± 6.6	127.7	113.1 ± 10.6	90.8	82.6 ± 11.4	72.8
0.80	296.9 ± 19.9	324.0	254.1 ± 12.7	242.1	188.7 ± 17.7	171.6	139.7 ± 19.4	124.4
1.00	395.3 ± 25.7	406.7	341.2 ± 17.2	319.1	287.5 ± 27.0	241.8	190.5 ± 11.2	167.7
1.50	658.4 ± 19.8	724.2	545.3 ± 27.3	553.4	474.8 ± 19.0	437.6	329.2 ± 20.1	304.6
2.00	912.1 ± 27.4	1018.7	801.2 ± 34.4	787.8	678.4 ± 27.1	606.6	478.5 ± 28.2	470.1
3.00	1437.7 ± 43.1	1610.5	1272.6 ± 54.7	1313.2	1089.9 ± 43.6	1084.0	792.5 ± 46.7	780.5
4.00	1978.8 ± 59.4	2189.6	1684.0 ± 72.4	1825.8	1503.5 ± 60.1	1497.1	1243.9 ± 73.4	1178.4
5.00	2514.6 ± 75.4	2738.4	2142.9 ± 92.1	2338.2	1856.9 ± 74.3	1951.0	1601.5 ± 94.5	1510.0

Table I, is not possible at present. However, the trends of the measured positron transmission[5,9,18] on the energy and the atomic number of absorbing material are similar to the plots of R_p^+ vs T and Z (see Fig. 7).

To gain an idea about the reduction in the csda range due to the inclusion of multiple-scattering effect as described in this paper, the ratios of $R_p^-(T)/R^-(T)$ and $R_p^+(T)/R^+(T)$ versus energy T in Al, Cu, Ag, and Au are displayed in Fig. 8. It is clear that this ratio for a material is constant within ±4% for electrons and positrons, provided T is smaller than twice the rest of the mass energy of electron, which is in agreement with the scaling law of electron transport.[27] Beyond 1.0 MeV, this ratio increases with increasing energy and atomic number. This conclusion is strongly favored by a precise experiment on electron transmission by Spanel *et al.*[19] (for direct comparison, see Fig. 10 of Ref. 19), and the Monte Carlo calculations (for comparison, see Fig. 3 of Ref. 28) of $R_{ex}^-(T)/R^-(T)$ in Al and Cu reported by Perkins.[28]

The experimental ratio of R_{ex}^+ at 1.88 MeV to R_{ex}^- at 1.77 MeV in graphite, Al, Cu, Y, Sn, Nd, Ho, Yb, and Pb as reported by Takhar[12–14] has been compared with our calculations (see Fig. 9). One finds that the calculated ratio R_p^+/R_p^- agrees very well with the measured ratio R_{ex}^+/R_{ex}^- in Al, Cu, Sn, Yb, and Pb. But, there is a large difference in the case of graphite, Y, Nd, and Ho. The exact reason for this large difference, particularly, in the rare-earth materials and gra-

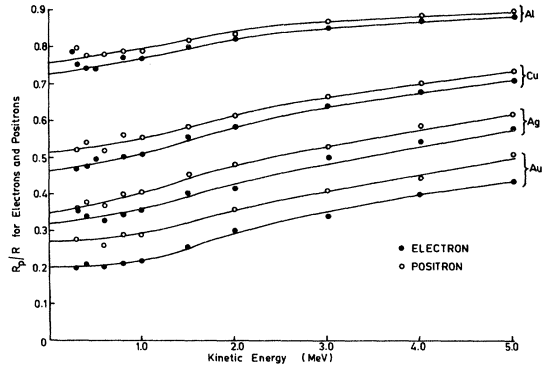

FIG. 8. Ratio of practical range R_p according to Eq. (2) to the csda range according to Eq. (1) of electron (●) and positron (○) in Al, Cu, Ag, and Au.

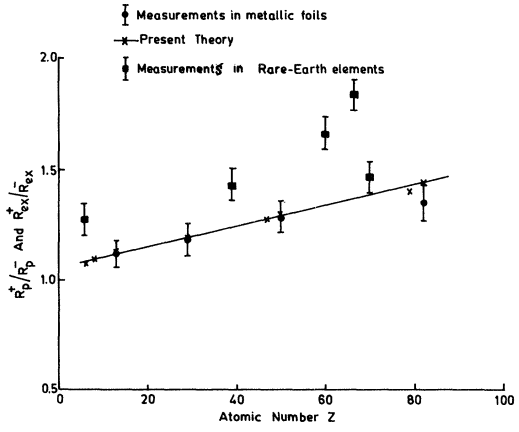

FIG. 9. Ratio of positron range at 1.88 MeV to electron range at 1.77 MeV as a function of atomic number. R_p^+/R_p^- calculated (*), R_{ex}^+/R_{ex}^- experimental (♦) in metallic foils and (■) in rare-earth elements and graphite (Refs. 12–14).

phite is not yet known. However, it is to be noted that graphite, Y, Nd, and Ho have different crystal structure than pure Al, Cu, Sn, Yb, and Pb. The detailed calculations regarding the effect of crystal structure on the ranges of electrons and positrons are in progress and would be published later. Furthermore, the similar measurements of positron range at 324 keV to electron range at 312 keV by Patrick and Rupaal,[29] in Al, Cu, Sn, and Pb also agree well with the present calculations.

Thus, we infer that the effect of multiple scattering on the penetration of electrons and positrons is to shorten the total path length (the csda range) in a material. And, the overall difference between the electron range and the positron range arises due to the differences in their total stopping powers and the multiple scattering cross sections for a given atomic number.

[1]J. Marshall and A. J. Wood, Can. J. Res. A 15, 39 (1937).
[2]F. L. Hereford and C. P. Swann, Phys. Rev. 78, 727 (1950).
[3]H. H. Seliger, Phys. Rev. 88, 408 (1952).
[4]H. H. Seliger, Phys. Rev. 100, 1029 (1955).
[5]L. Katz and A. S. Penfold, Rev. Mod. Phys. 24, 28 (1952).
[6]K. Gubernator, Z. Phys. 152, 183 (1958).
[7]K. Gubernator and A. Flammerfeld, Z. Phys. 156, 176 (1959).
[8]B. N. C. Abu, T. A. Burdett, and E. Matsukawa, Proc. Phys. Soc. 72, 727 (1958).
[9]V. E. Cosslett and R. N. Thomas, Brit. J. Appl. Phys. 15, 883 & 1283 (1964).
[10]P. J. Elbert, A. F. Lauzon, and E. M. Lent, Phys. Rev. 183/2, 4222 (1969).
[11]T. Tabata, R. Ito, and S. Okabe, Nucl. Instrum. Methods 103, 85 (1972).
[12]P. S. Takhar, Phys. Rev. 157, 257 (1967).
[13]P. S. Takhar, Phys. Lett. 28, 423 (1968).
[14]P. S. Takhar, Phys. Lett. 23, 219 (1966).
[15]M. J. Berger and S. M. Seltzer, National Research Council Publ. No. 1133, 205–268 (1964).
[16]R. K. Batra and M. L. Sehgal, Nucl. Phys. A 156, 314 (1970).
[17]R. K. Batra and M. L. Sehgal, Nucl. Phys. A 196, 638 (1972).
[18]R. K. Batra and M. L. Sehgal, Nucl. Instrum. Methods 109, 565 (1973).
[19]L. E. Spanel, A. S. Rupaal, and J. R. Patrick, Phys. Rev. B 8, 4072 (1973).
[20]N. F. Mott, Proc. R. Soc. London Ser. A 124, 425 (1929).
[21]E. J. Williams, Proc. R. Soc. London Ser. A 169, 531 (1939).
[22]H. S. W. Massey, Proc. R. Soc. London Ser. A 181, 14 (1943).
[23]W. H. McKinley and H. Feshbach, Phys. Rev. 74, 1759 (1948).
[24]R. Rossi and X. Greisen, Rev. Mod. Phys. 13, 262 (1941).
[25]T. Scott Williams, Rev. Mod. Phys. 35/2, 231 (1963).
[26]S. R. Thantadarya and N. Umakantha, Phys. Rev. B 4, 1632 (1971).
[27]C. H. Blanchard and U. Fano, Phys. Rev. 82, 767 (1951).
[28]J. F. Perkins, Phys. Rev. 126, 1781 (1962).
[29]J. R. Patrick and A. S. Rupaal, Phys. Lett. A 35, 235 (1971).